Chemistry Letters

Quinoxalineimide as a Novel Electron-Accepting Building Block for Organic Optoelectronics

Tsukasa Hasegawa, Koutarou Aoyagi, Minoru Ashizawa,* Yuichi Konosu, Susumu Kawauchi, Niyazi Sedar Sariciftci, and Hidetoshi Matsumoto*

Advance Publication on the web May 26, 2015 by J-STAGE

doi:10.1246/cl.150407

Quinoxalineimide as a Novel Electron-Accepting Building Block for Organic Optoelectronics

Tsukasa Hasegawa, [1] Koutarou Aoyagi, [1] Minoru Ashizawa,*[1] Yuichi Konosu, [1] Susumu Kawauchi, [1]
Niyazi Sedar Sariciftci, [2] and Hidetoshi Matsumoto *[1]
[1]*Department of Organic and Polymeric Materials, Tokyo Institute of Technology, 2-12-1 Ookayama, Meguro-ku, Tokyo 152-8552*
[2]*Linz Institute for Organic Solar Cells (LIOS), Johannes Kepler University Linz, Altenbergerstraße 69, 4040 Linz, Austria*

E-mail: matsumoto.h.ac@m.titech.ac.jp

Organic semiconductors with a donor-acceptor-donor architecture based on the novel acceptor unit of quinoxalineimide (QI) were designed and synthesized. They absorbed wider wavelength light compared to $PC_{61}BM$, and functioned as acceptor materials for solution-processed bulk-heterojunction organic photovoltaic devices. In addition, the relatively shallow LUMO levels, due to the electron-withdrawing pyrazine and imide groups of the QI unit, resulted in a high open circuit voltage of the devices.

Organic semiconductors have received enormous attention over the past decade since they have unique optoelectronic properties such as strong light absorption, light emission and charge transport. They are widely investigated as the active materials in organic field effect transistors (OFETs), organic photovoltaics (OPVs), and organic light emitting diodes (OLEDs).[1] Among the organic semiconductors, electron-rich π-conjugated building blocks serving as electron donors have been well studied in organic electronics.[2] However, the development of electron-deficient π-conjugated systems is still lacking relative to the electron-rich counterpart, which limits their application in complemental logic circuits and OPVs using an alternative acceptor to replace the [6, 6]-phenyl C_{61} and C_{71} butyric acid methyl esters ($PC_{61}BM$ and $PC_{71}BM$).[3] Therefore, novel electron-accepting building blocks are highly required both in small molecular and polymeric materials.[4]

In the present study, we first designed the quinoxalineimide (QI) unit, which contains the electron-withdrawing pyrazine and imide groups, as shown in Figure 1. The fusing of the pyrazine ring with the imide makes the LUMO level deeper than that of the naphthalene imide (Figure S1). The alkyl chains at the imide position of the QI unit improve the solubility and film forming ability. In addition, chemical modification through the 5- and 8-positions of the quinoxaline group enables the π-conjugated connection to form oligomeric and polymeric backbones. We used the QI unit as a strong electron-accepting building block and synthesized new thiophene-flanked quinoxalineimide (QI) small molecules, i.e., QI-Th and QI-BiTh, to form donor-acceptor-donor (D-A-D) molecules, in which the D-A connection is useful for tailoring frontier molecular orbitals on individual devices.

In order to examine the versatility of the electron-accepting building block of the QI unit, we investigated the properties of QI-Th and QI-BiTh and used them as an electron acceptor in bulk-heterojunction OPV devices with the poly(3-hexylthiophene) (P3HT) electron donor. Compared to the benchmark device composed of P3HT and $PC_{61}BM$, the obtained power conversion efficiencies around 0.3% of QI-Th and QI-BiTh are low, but with higher open-circuit voltage (V_{oc}) values due to the QI unit are achieved. These results nicely demonstrate that the novel QI building block is potentially an active component in organic devices.

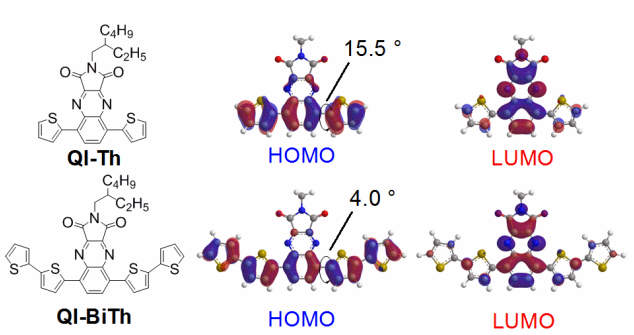

Figure 1. Chemical structure and pictorial representations of the frontier molecular orbitals of QI derivatives with two dihedral angles obtained by DFT calculations.

The common pathway toward the QI unit is shown in Scheme S1. The detailed synthetic procedures and characterization data are described in the Supporting Information. We carried out the reactions at room temperature or under gentle reflux conditions to prepare the QI unit since the 2- and 3-positions are active for nucleophile attack, and preparation of QI unit sometimes suffered from the disappearance of the carboxylic groups at elevated temperatures. The thiophene-flanked QI molecules, QI-Th and QI-BiTh, were synthesized via the Stille coupling reaction.[5] Both compounds were readily soluble in the common organic solvents such as chloroform, toluene and chlorobenzene. The thermal stability of the QI derivatives was investigated by a thermogravimetric analysis (TGA) (Figure S2), and the thermal transition temperatures of the QI derivatives were also investigated by differential scanning calorimetry (DSC) (Figure S3). The 5% degradation temperature ($T_{d5\%}$), the melting temperature (T_m) and crystallization temperature (T_c) are summarized in Table S1. Both compounds are thermally stable up to 300 °C, which is a sufficient thermal stability to improve the film morphology for the OPV device.

To investigate the electronic properties and the geometries of the QI derivatives, quantum chemical calculations were performed using the DFT/B3LYP/6-31G+(d,p) method. In the optimized geometries of the molecules (Figure 1), the two dihedral angles of QI-Th and QI-BiTh are 15.5° and 4.0°, respectively. QI-BiTh prefers more planar conformation than QI-Th probably due to extended π-conjugation. For these molecules, the π-electrons in the HOMO orbitals are delocalized on the lateral conjugated

backbone along the thiophene connection. On the other hand, the LUMO orbitals are localized over the QI moiety due to the electron-withdrawing character of pyrazine and imide groups of the QI unit. The calculated HOMO/LUMO energy and energy gaps (E_g^{cal}) of the QI derivatives are summarized in Table S2. The QI derivatives have relatively shallow LUMO energies close to −3.2 eV. It is also estimated that QI-BiTh has a higher HOMO energy and narrower band gap than QI-Th, thus QI-BiTh can have a wider light absorption band than QI-Th.

The electrochemical property of the QI derivatives was investigated by cyclic voltammetry (CV). The results revealed that both QI-Th and QI-BiTh exhibited amphoteric redox behaviors (Figure S4). The HOMO/LUMO energy obtained from the cyclic voltammograms and energy gap (E_g) are summarized in Table 1. The HOMO/LUMO energies were calculated from the onset oxidation potentials (E^{ox}_{onset}) and onset reduction potentials (E^{red}_{onset}), respectively, based on the following equations: $E_{HOMO}=-[E^{ox}_{onset}-E_{1/2}(Fc/Fc^{+})+4.8]$V; $E_{LUMO}=-[E^{red}_{onset}-E_{1/2}(Fc/Fc^{+})+4.8]$V, in which the potentials refer to the $Ag/AgNO_3$ reference electrode.[6] The LUMO energies of both QI derivatives are comparable as estimated values from the theoretical calculations. The LUMO energy around −3.5 eV is an intermediate value between the common donor material P3HT and common accepter material $PC_{61}BM$. Therefore, it is predicted that these QI derivatives can act as either an acceptor or donor material. On the other hand, the HOMO energy of QI-BiTh rose and the energy gap narrowed to 1.47 eV from 2.00 eV, as estimated from the theoretical calculations. Based on this result, it is expected that the onset value of the light absorption band of QI-BiTh reached a longer wavelength than that of QI-Th. As generally accepted, the built-in potential is directly related to the maximum V_{oc} value of the OPV devices, which can be estimated by the energy difference between the HOMO energy of the donor material and LUMO energy of the acceptor.[7] Compared to the P3HT:$PC_{61}BM$ with the built-in potential of 1.4 eV, the QI derivatives:P3HT exhibit a higher built-in potential (1.6 eV). Thus the OPV devices based on the QI derivatives as an acceptor material are expected to show a high V_{oc} value.

Table 1 Electrochemical properties of QI derivatives.

	HOMO /eV	LUMO /eV	E_g [a] /eV
QI-Th	-5.55[c]	-3.55[b]	2.00
QI-BiTh	-4.98[b]	-3.51[b]	1.47
$PC_{61}BM$	-5.72[b]	-3.71[b]	2.01

[a] Energy gaps were calculated from (LUMO−HOMO). [b] The data were obtained from cyclic voltammogram in 0.1 M 1,2-dichlorobenzene/n-Bu_4NPF_6 solution at the scan rate of 100 mV s^{-1}, $HOMO=-[E^{ox}_{onset}-E_{1/2}\ (Fc/Fc^{+})+4.8]$; $LUMO=-[E^{red}_{onset}-E_{1/2}\ (Fc/Fc^{+})+4.8]$. [c] In 0.1 M THF/n-$Bu_4NPF_6$ solution.

To characterize the optical properties of the QI derivatives, the UV-vis absorption spectroscopy of the molecules were performed both in a dilute solution and thin films. Figure 2a shows the absorption spectra of the QI derivatives in dilute chloroform solutions ($(1–5)\times10^{-5}$ M), and their maxima wavelengths (λ_{max}) are summarized in Table S3. The QI derivatives have two absorption bands; higher absorption bands (with maxima at *ca.* 320 and 373 nm) and lower ones (with maxima at *ca*. 500 and 575 nm). From the TD-DFT estimation, the former bands correspond to the HOMO-LUMO+2 transition, and the latter ones correspond to the π–π* transition (Table S4). A significant red-shift in the absorption maximum of QI-BiTh relative to that of QI-Th is observed, consequently, the absorption band of QI-BiTh is much wider than that of $PC_{61}BM$. The absorption spectra of the QI derivatives in the thin films are shown in Figure 2b, and the λ_{max} and optical band gap (E_g^{opt}) are summarized in Table S3. These spectra were normalized at the maximum of the bands corresponding to the π–π* transition. The significant red-shift of the absorption spectra in the thin films compared to that in solution can be attributed to the planarization of the molecules forming intermolecular interactions in the solid state. Compared to QI-Th, QI-BiTh showed a significant red-shift in the absorption band with the absorption band edge reaching 770 nm, which is due to the narrower energy gap of QI-BiTh. The E_g^{opt} values of the QI derivatives, which were calculated from the onset wavelengths, were 1.97 and 1.61 eV. These values are closely related to the energy gap obtained from the cyclic voltammograms.

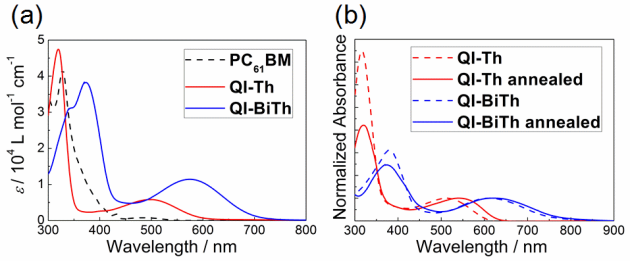

Figure 2. UV-vis absorption spectra of QI derivatives (a) in $CHCl_3$ and (b) in spin-coated film (normalized by absorbance at the top of band correspond to the π–π* transition, dot line: as-cast films, solid line: annealed films at 100 ºC for 10 min).

To evaluate the carrier transporting property of the QI derivatives, we carried out space charge limited current (SCLC) measurements. Based on the SCLC fitting of the dark current density-voltage (*J-V*) curves (Figure S5), QI-Th showed an electron transporting ability, and its electron mobility is 2.6×10^{-7} cm^2 V^{-1} s^{-1}, while QI-Th did not show a hole transporting ability. This would be attributed to the smaller donor unit constituting the HOMO distribution along the flanked thiophenes, then the effective hole transport path was not formed. On the other hand, QI-BiTh showed an ambipolar nature, its electron- and hole-mobilities being 5.8×10^{-7} and 10.0×10^{-7} cm^2 V^{-1} s^{-1}, respectively. The above findings demonstrate that QI-BiTh possesses an appropriate energy level and charge transporting characteristic for either the acceptor or donor material.

Solution-processed OPV devices were fabricated and optimized with the structure of ITO/cross-linked polyethyleneimine (PEI)/active layer/MoO_3/Ag.[8] The *J-V* curves of the OPV devices are shown in Figure 3. The donor/acceptor weight ratio of the active layer on the performance of the OPV devices was optimized. The photovoltaic parameters calculated from the *J-V* curves, including the open-circuit voltage (V_{oc}), short-circuit current density (J_{sc}), and fill factor (*FF*), are summarized in Table 2. The OPV devices based on QI-Th:P3HT (1:2 w/w) and QI-

BiTh:P3HT (1:1 w/w) as the active layer were fabricated to estimate the potential of the novel QI derivatives as a novel acceptor material. The devices showed the higher V_{oc} values of 0.80 and 0.85 V than that of the PCBM:P3HT device, well agreeing with high built-in potentials of QI-Th and QI-BiTh. Consequently, the device based on the QI-BiTh acceptor having the higher V_{oc} of 0.85 V produced the higher power conversion efficiency (PCE) of 0.34% with a V_{oc} of 0.85 V, J_{sc} of 0.91 mA cm^{-2}, FF of 0.35. The OPV devices based on the QI-derivative:$PC_{61}BM$ as the active layer were also fabricated to investigate the ambipolar characteristic for OPV since QI-Th and QI-BiTh provide the driving force above 0.3 eV required for charge-transfer from P3HT to QI-Th and QI-BiTh.[9] QI-Th did not act as a donor material due to the absence of its hole transporting ability. In contrast, QI-BiTh acted as a donor material and the device based on it showed the power conversion efficiency (PCE) of 0.38% with a V_{oc} of 0.63 V, J_{sc} of 1.57, and *FF* of 0.31. The low J_{sc} values of the devices are mainly due to the morphology of the active layer. The AFM image (Figure S6), carrier mobilities of the OPV devices measured by the SCLC method (Table S5) and detailed discussions are included in the Supporting Information.

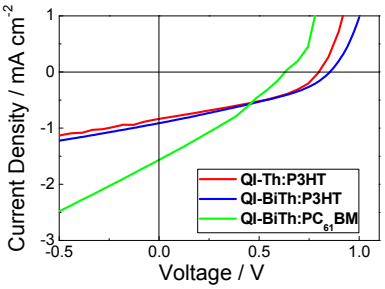

Figure 3. Current density-voltage curves of OPV devices based on QI derivatives under AM 1.5 G.

Table 2 OPV properties of QI derivatives.

	V_{oc} /V	J_{sc} /mA cm^{-2}	FF /-	PCE_{max}(PCE_{ave}) /%
QI-Th:P3HT (1:2 w/w)[a]	0.80	0.84	0.39	0.33 (0.29)
QI-BiTh:P3HT (1:1 w/w)[a]	0.85	0.91	0.35	0.34 (0.31)
QI-BiTh:$PC_{61}BM$ (1:2 w/w)[a]	0.63	1.57	0.31	0.38 (0.35)
P3HT:$PC_{61}BM$ (3:2 w/w)[a]	0.63	8.35	0.65	3.38 (3.34)

[a] Device structure: ITO/cross-linked PEI/ active layer /MoO_3/Ag.

The absorption spectra and the external quantum efficiency (EQE) spectra of these devices are shown in Figure 4. The photo-response curves agreed with the absorption spectra of the QI-derivative:P3HT blended films. On the other hand, the shape of the EQE spectra of the QI-BiTh:$PC_{61}BM$ is different from the absorption spectra. It is similar to the absorption spectra of QI-BiTh (Fig. 2b). This implies that QI-BiTh mainly contributes to the photocurrent. The EQE spectra demonstrate that QI-BiTh can convert a wide wavelength light up to ca. 770 nm to a photocurrent.

In summary, novel organic semiconductors, small molecules with a D-A-D architecture containing the unprecedented acceptor unit of QI with flanked thiophenes as the donor unit, — QI-Th and QI-BiTh — have been

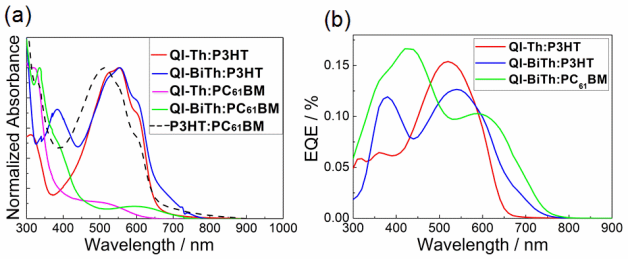

Figure 4. (a) UV-vis absorption spectra of active layers based OPV devices. (b) EQE spectra of the OPV devices based on QI derivatives.

synthesized and characterized. The QI-BiTh exhibited a wider absorption band than QI-Th due to its narrower band gap. Consequently, QI-BiTh absorbs the longer wavelength light compared to $PC_{61}BM$. Compared with the P3HT:$PC_{61}BM$ blend, the QI derivatives exhibit a higher built-in potential (1.6 eV) blended to form acceptor materials with P3HT. These results indicated that the QI based organic semiconductors with the D-A-D architecture are promising acceptors with a wide absorption band and high cell V_{oc} value for the solution-processed OPV. In addition, QI-BiTh also acted as a donor material. This ambipolar property indicates the potential of precise tuning of the energy levels of QI-based organic semiconductors. The molecular design of oligomeric and polymeric semiconductors using the QI electron-accepting building unit is being pursued to enhance the charge transfer and control phase-separated morphology.

The authors thank Dr. Matthew White and Mr. Patrick Denk (Linz Institute for Organic Solar Cells, Johannes Kepler University Linz) for providing valuable comments and technical support for this study. This study was partly supported by a Grant-in-Aid for Scientific Research (C) (No. 26410087) from the Ministry of Education, Culture, Sports, Science and Technology. The numerical calculations were carried out on the TSUBAME2.5 supercomputer at the Tokyo Institute of Technology, Japan, and on the supercomputer in the Research Center for Computational Science, Japan.

Supporting Information is available electronically on J-STAGE.

References and Notes

1 (a) A. R. Murphy, J. M. J. Fréchet, *Chem. Rev.*, **2007**, *107*, 1066. (b) A. W. Hains, Z. Liang, M. A. Woodhouse, B. A. Gregg, *Chem. Rev.*, **2010**, *110*, 6689.
2 J. Roncali, P. Leriche, P. Blanchard, *Adv. Mater.*, **2014**, *26*, 3821.
3 (a) Y. Lin, Y. Li, X. Zhan, *Chem. Soc. Rev.*, **2012**, *41*, 4245. (b) J. E. Anthony, A. Facchetti, M. Heeney, S. R. Marder, X. Zhan, *Adv. Mater.*, **2010**, *22*, 3876.
4 K. Aoyagi, Y. Shoji, S. Otsubo, S. Kawauchi, M. Ueda, H. Matsumoto, T. Higashihara, *Bull. Chem. Soc. Jpn.*, **2014**, *87*, 1083.
5 D. Milstein, J. K. Stille. *J. Am. Chem. Soc.*, **1978**, *100*, 3636.
6 A. Takahashi, C. J. Lin, K. Ohshimizu, T. Higashihara, W. C. Chen, M. Ueda, *Polym. Chem.* **2012**, *3*, 479.
7 C. J. Brabec, A. Cravino, D. Meissner, N. S. Sariciftci, T. Fromherz, M. T. Rispens, L. Sanchez, J. C. Hummelen, *Adv. Funct. Mater.* **2001**, *11*, 374.
8 Y. Udum, P. Denk, G. Adam, D. H. Apaydin, A. Nevosad, C Teichert, M. S. White, N. S. Sariciftci, M. C. Scharber, *Org. Electron.* **2014**, *15*, 997.
9 (a) T. M. Clarke, J. R. Durrant, *Chem. Rev.*, **2010**, *110*, 6736 (b) B. Walker, A. B. Tamayo, X.-D. Dang, P. Zalar, J. H. Seo, A. Garcia, M. Tantiwiwat, T.-Q. Nguyen, *Adv. Funct. Mater.*, **2009**, *19*, 3063.